Mechanism of improvement of formability in pulsating hydroforming of tubes

K. Mori*, T. Maeno, S. Maki

Department of Production Systems Engineering, Faculty of Engineering, Toyohashi University of Technology, Tempaku-cho, Toyohashi, Aichi 441-8580, Japan

Abstract

The mechanism of improvement of formability by the oscillation of internal pressure in a pulsating hydroforming process of tubes was examined. Free bulging hydroforming experiments of mild steel tubes under oscillating and constant inner pressures were performed. For a high constant pressure, a round bulge with local thinning was observed, whereas wrinkling occurred for a low constant pressure. The occurrence of these defects was prevented by oscillating the internal pressure in the pulsating hydroforming. In the pulsating hydroforming, a uniform expansion in the bulging region was obtained, and thus the formability was improved by preventing the local thinning. It was found from an observation of deformation behaviour, using a video camera, that the tube is uniformly expanded by repeating the appearance and disappearance of small wrinkling. The cause of the uniform expansion for the pulsating hydroforming was also interpreted from the variation of stress components. In addition, a similar deference in deformation behaviour between the oscillating and constant inner pressures was also obtained in finite element simulation.
© 2006 Elsevier Ltd. All rights reserved.

Keywords: Tube forming; Pulsating hydroforming; Pressure oscillation; Free bulging; Formability; FEM simulation

1. Introduction

For the reduction in weight of automobiles, hollow products are increasingly employed for automobile parts. Since the bending stiffness of the hollow products is larger than that of the solid products under the same weight, the hollow products are effective in the reduction in weight. The hydroforming of tubes is attractive in automobile industry as a forming process of hollow products. In the hydroforming process, the tube is bulged by the internal pressure to be formed into a desired shape with dies. The wall thickness of the tube is decreased by the bulging, and thus this brings about the bursting of the tube. The decrease in wall thickness is prevented by compressing the tube in the axial direction simultaneously with the action of the internal pressure. For the axial compression, the wrinkling of the tube results from an excessively small pressure. The paths of internal pressure in the tube hydroforming are a key to preventing the occurrence of these defects. The finite element simulation has been employed to determine the pressure paths [1–5].

For the forming of hollow products with a complex shape, a pulsating hydroforming process of tubes has been developed [6]. In this process, the internal pressure necessary for the bulging of the tube is oscillated during the hydroforming. The authors [7] have investigated the improvement of the formability by means of the pulsating hydroforming. Hama et al. [8] have simulated a pulsating hydroforming process of a three-dimensional automotive part by the finite element method. The deformation behaviour of the tube in the hydroforming is greatly influenced by the friction at the interface between the tube and die [9]. Although the friction during forming is reduced by ultrasonic vibration of dies [10], the friction in the pulsating hydroforming has been hardly decreased by the oscillation of internal pressure [11]. Since the frequency of the ultrasonic vibration is much higher than that of the

*Corresponding author. Tel.: +81 532 44 6707; Fax: +81 532 44 6690.
E-mail address: mori@plast.pse.tut.ac.jp (K. Mori).

pulsating hydroforming, the pulsating hydroforming may have a different mechanism for improving the formability from the change in friction.

In the present study, a mechanism of improvement of formability by the pulsating hydroforming was examined from an observation of deformation behaviour. Results in a free bulging hydroforming experiment for the oscillating inner pressure were compared with those for constant pressures.

2. Hydroforming procedure

Deformation behaviour of tubes during the hydroforming was observed in a free bulging hydroforming experiment of mild steel tubes. The free bulging hydroforming having a bulging region in no contact with a die shown in Fig. 1 was chosen to examine the effect of the oscillation of internal pressure on the bulging behaviour. In this experiment, the die set was installed in a screw driven type universal testing machine, and the tube was compressed by moving the upper punch downward with the universal testing machine under the fixture of the lower punch. The pressure was generated by a hydraulic pump and was transmitted with a water-oil emulsion through the lower punch. The outer diameter, wall thickness and length of the tube were 38.1, 1.1 and 200 mm, respectively. Both sides in contact with the upper and lower dies were lubricated with a water-soluble press oil.

The path of internal pressure for the pulsating hydroforming shown in Fig. 2 is expressed by

$$p = \Delta p \sin 2\pi\omega(s - 1.5) + p_0, \tag{1}$$

where Δp is the amplitude of the cycle of the pressure, ω is the number of cycles per unit punch stroke and s is the stroke of the upper punch. The pulsating pressure was oscillated from the base pressure p_0, and the oscillation started from $s = 1.5$ mm. The tube was compressed under a
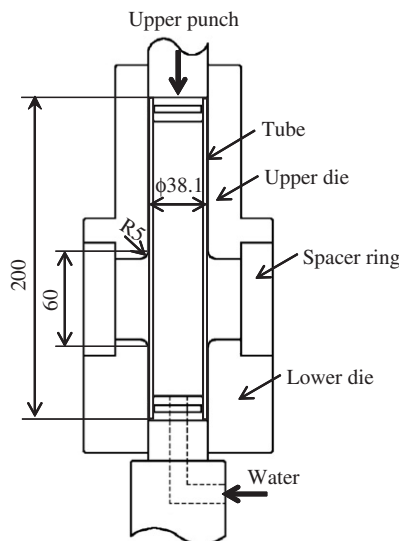

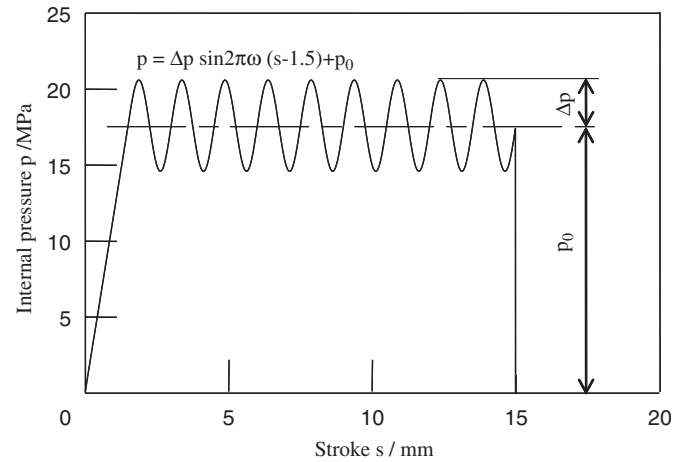Fig. 1. Tools used in free bulging hydroforming experiment of tube.

Fig. 2. Oscillation of internal pressure in pulsating hydroforming of tube.

constant velocity of the upper punch of 1.5 mm/s, and thus the path of axial force for the compression of the tube was obtained as a result of the experiment. It is noted that the tube continues to undergo plastic deformation during the hydroforming due to the continuous compression in the axial direction, i.e. the deformation is plastic even in the drop of internal pressure of the oscillation.

3. Results of hydroforming experiment

The hydroformed tube for $p_0 = 17.7$ MPa, $\Delta p = 3$ MPa, $\omega = 0.67$ c/mm in the pulsating pressure is compared with those for the constant pressures in Fig. 3. The round bulge and wrinkling occur for the high and low constant pressures, respectively, whereas the uniform expansion having an even top of the bulging region appears for the pulsating pressure. The uniform expansion is hardly observed in the conventional hydroforming processes.

The distributions of wall thickness strain in the bulging region for the three pressure paths are shown in Fig. 4. The wall thickness was measured without cutting the hydroformed tube by means of an ultrasonic instrument corrected by a micrometre. For the high constant pressure, the wall thickness in the centre of the bulging region becomes small due to the tension, i.e. the local thinning, and the wall thickness for the low constant pressure waves. On the other hand, the wall thickness around the centre of the bulging region uniformly decreases for the pulsating pressure, and thus the formability is improved by the uniform expansion without the local thinning.

The effect of the base pressure on the shape of the bulging region for $\Delta p = 3$ MPa and $\omega = 0.67$ c/mm in the pulsating pressure is given in Fig. 5. The shape of the bulging region was measured by means of a laser sensor. The uniform expansion is obtained for $p_0 = 17.7$ MPa, whereas the round bulging and wrinkling occur for the high and low base pressures, respectively. The pulsating hydroforming has an optimum base pressure for the uniform expansion.
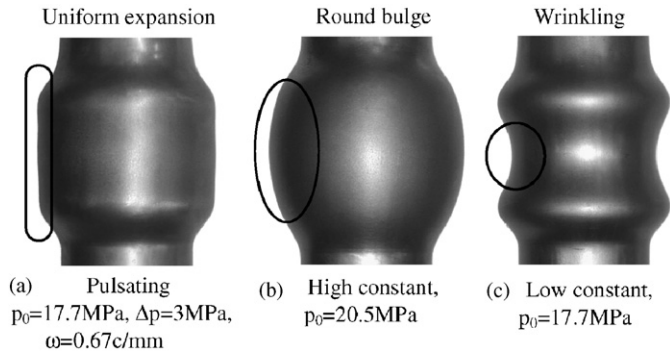
(a) Pulsating
$p_0 = 17.7$ MPa, $\Delta p = 3$ MPa, $\omega = 0.67$ c/mm

(b) High constant, $p_0 = 20.5$ MPa

(c) Low constant, $p_0 = 17.7$ MPa

Fig. 3. Hydroformed tubes obtained from experiment for three pressure paths.

The effect of the number of cycles on the shape of bulging region for $p_0 = 17.7$ MPa and $\Delta p = 3$ MPa in the pulsating pressure is shown in Fig. 6. Although the effect of the number of cycles is smaller than that of the base pressure, the decrease in the number tends to cause the wrinkling.

The relationships between the curvature in the centre of the bulging region and the base pressure for different amplitudes of cycle of pressure are illustrated in Fig. 7. As the curvature approaches 0, the centre of the bulging region becomes even, i.e. the curvature within ± 0.01/mm is equivalent to the even surface. The constant pressure represented by $\Delta p = 0$ MPa has no date of curvature within ± 0.01/mm, and the curvatures within the limit are

Fig. 4. Distributions of wall thickness strain in bulging region for three pressure paths (pulsating: $p_0 = 17.7$ MPa, $\Delta p = 3$ MPa, $\omega = 0.67$ c/mm, High constant: $p_0 = 20.5$ MPa, Low constant: $p_0 = 17.7$ MPa).
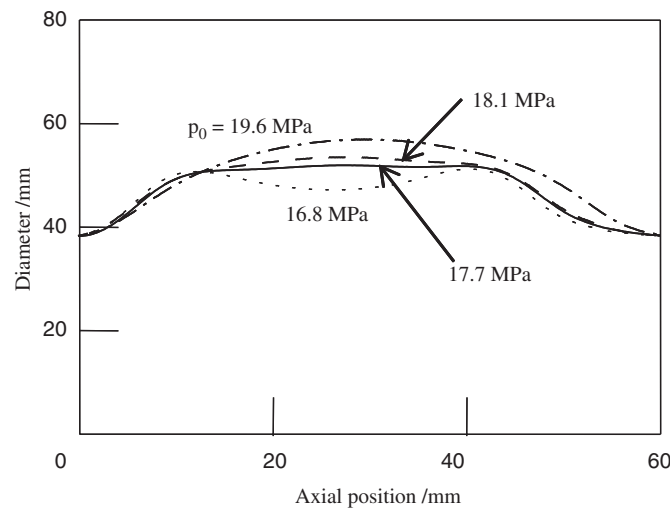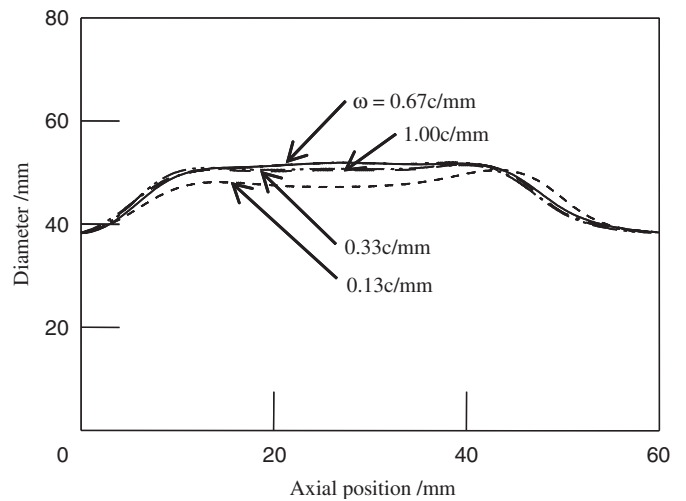

Fig. 6. Effect of number of cycles on shape of bulging region for $p_0 = 17.7$ MPa and $\Delta p = 3$ MPa in pulsating pressure.

Fig. 5. Effect of base pressure on shape of bulging region for $\Delta p = 3$ MPa and $\omega = 0.67$ c/mm in pulsating pressure.
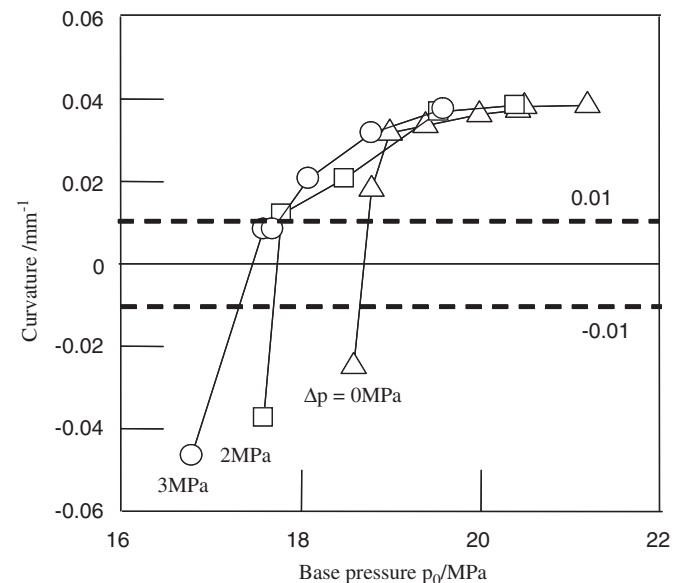

Fig. 7. Relationships between curvature in centre of bulging region and base pressure for different amplitudes of cycle.

obtained for the pulsating pressure of $\Delta p = 3\,\text{MPa}$. Although it is difficult to observe the uniform expansion in the conventional hydroforming due to the narrow range of the pressure, the uniform expansion appears for the pulsating hydroforming because of the wide range of the base pressure.

4. Mechanism for improvement of formability

4.1. Deforming shape

In the pulsating hydroforming, the local thinning is prevented by the uniform expansion, and thus the formability is improved. Deformation behaviour of the tube during the hydroforming was observed by means of a video camera to examine a mechanism for exhibiting the uniform expansion.

The deforming shape of the bulging region for $p_0 = 17.7\,\text{MPa}$, $\Delta p = 3\,\text{MPa}$ and $\omega = 0.67\,\text{c/mm}$ in the pulsating pressure was shown in Fig. 8. The uniform expansion having an even top of the bulging region grows.

The deforming shape of the bulging region for the high constant pressure is given in Fig. 9. The round bulge grows unlike the pulsating hydroforming shown in Fig. 8.

The relationship between the deforming shape of the bulging region and the internal pressure for $p_0 = 17.7\,\text{MPa}$, $\Delta p = 3\,\text{MPa}$ and $\omega = 0.67\,\text{c/mm}$ in the pulsating pressure is illustrated in Fig. 10. Although small wrinkling appears
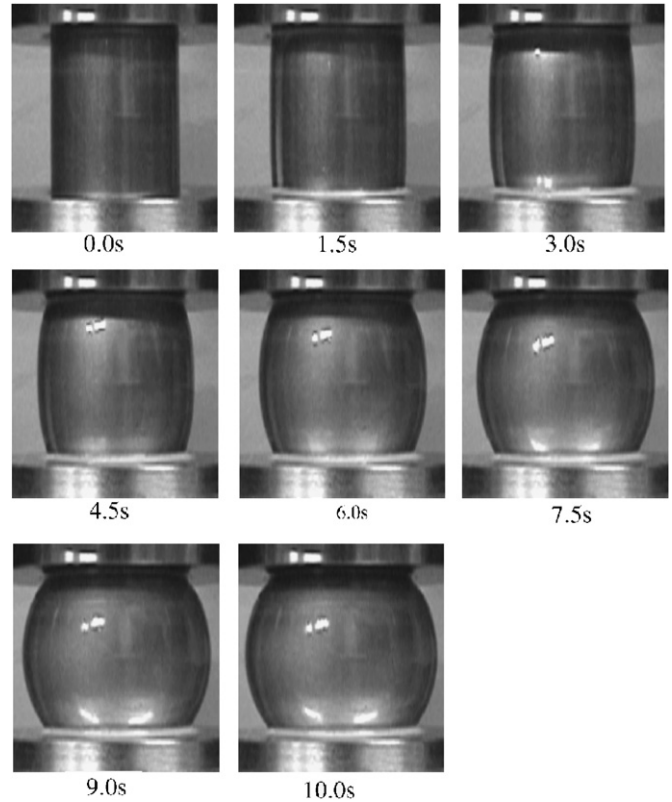

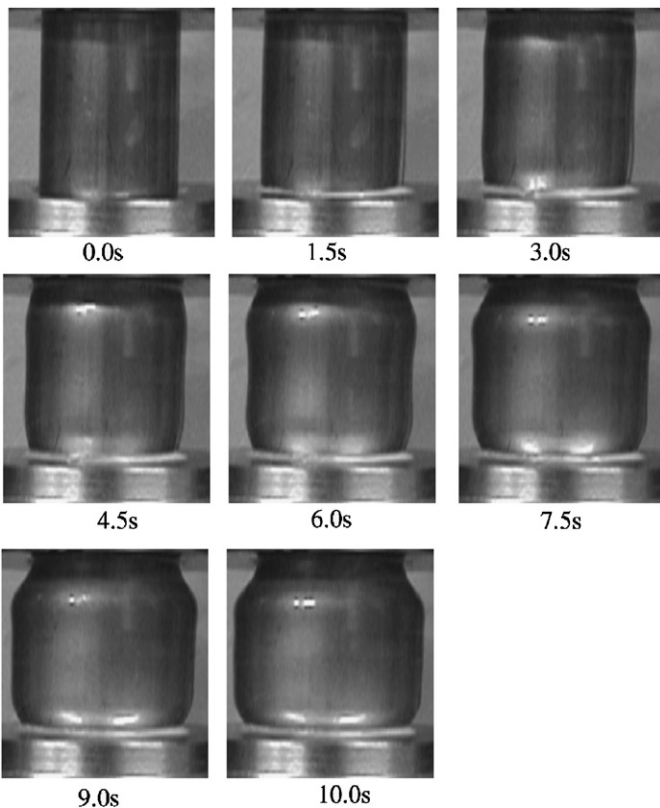Fig. 9. Deforming shape of bulging region for high constant pressure.
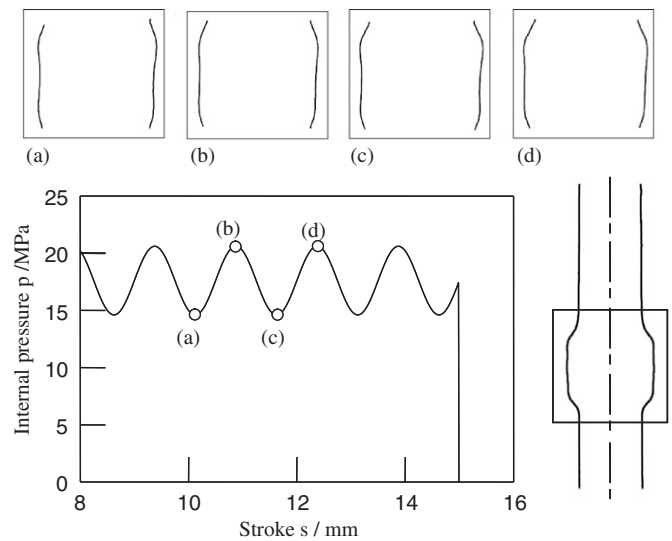

Fig. 10. Relationship between deforming shape of bulging region and internal pressure for $p_0 = 17.7\,\text{MPa}$, $\Delta p = 3\,\text{MPa}$ and $\omega = 0.67\,\text{c/mm}$ in pulsating hydroforming.

Fig. 8. Deforming shape of bulging region for $p_0 = 17.7\,\text{MPa}$, $\Delta p = 3\,\text{MPa}$ and $\omega = 0.67\,\text{c/mm}$ in pulsating pressure.

due to the decrease in pressure in Fig. 10(a), the wrinkling disappears due the increase in pressure in Fig. 10(b). In the pulsating hydroforming, the appearance and disappearance of the small wrinkling are repeated under the synchronisation with the change in pressure. The tube is uniformly expanded by repeating the appearance and

disappearance of the small wrinkling, and thus the local thinning is prevented.

4.2. Variation of stress

The stress components in the bulging region of the tube are influenced by the oscillation of internal pressure. Since the radial stress in the bulging region is p and 0 at the inner and outer surfaces, respectively, the average radial stress σ_r is approximated by

$$\sigma_r = -\frac{p}{2}. \tag{2}$$

By assuming a thin tube, the hoop stress σ_θ is expressed by

$$\sigma_\theta = \frac{pr}{t}, \tag{3}$$

where r and t are approximated to be the average of the initial inner and outer radii and the initial wall thickness, respectively. The average axial stress σ_z is calculated by

$$\sigma_z = -\frac{F_z}{2\pi rt}, \tag{4}$$

where F_z is the axial force for the compression of the tube. The axial force was obtained from the measured punch force F_p minus the force F_i for the action of the inner pressure inside the tube as shown in Fig. 11.

The oscillation of the axial force and internal pressure during the pulsating hydroforming for $p_0 = 17.7\,\text{MPa}$, $\Delta p = 3\,\text{MPa}$ and $\omega = 0.67\,\text{c/mm}$ is illustrated in Fig. 11. The axial force is synchronised with the internal pressure, i.e. the axial force exhibits peaks at the minimum inner pressures and the tendency for the maximum pressures is opposite.

The oscillation of the stress components in the bulging region calculated from Eqs. (2)–(4) during the pulsating hydroforming for $p_0 = 17.7\,\text{MPa}$, $\Delta p = 3\,\text{MPa}$ and $\omega = 0.67\,\text{c/mm}$ is given in Fig. 12, where the positive and

Fig. 12. Oscillation of stress components calculated from Eqs. (2)–(4) during pulsating hydroforming for $p_0 = 17.7\,\text{MPa}$, $\Delta p = 3\,\text{MPa}$ and $\omega = 0.67\,\text{c/mm}$.
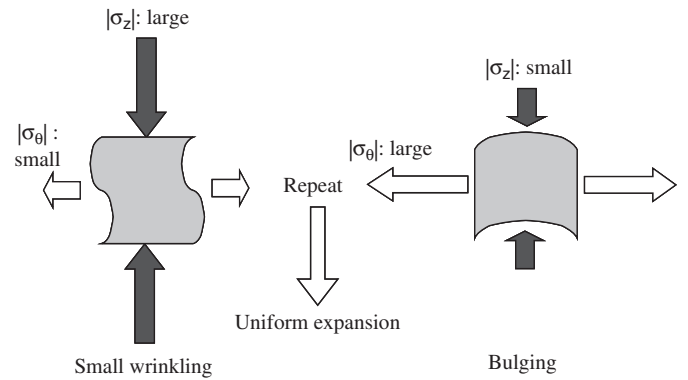
Fig. 13. Cause of uniform expansion in pulsating hydroforming by change in stress components.

negative signs denote tension and compression, respectively. The absolute value of σ_r is negligibly small in comparison with σ_θ and σ_z. Since σ_θ and σ_z are calculated from the inner pressure in Eq. (3) and the axial force in Eq. (4), respectively, σ_θ and σ_z are synchronised like Fig. 11. This synchronisation of the stress components is interpreted from plastic deformation of the tube. For a plastically deforming tube, the stress components obey the yield criterion. By substituting $\sigma_r = 0$ into the von Mises' yield criterion, we have

$$\bar{\sigma} = \sqrt{\frac{1}{2}\{(\sigma_\theta - \sigma_z)^2 + \sigma_\theta^2 + \sigma_z^2\}}. \tag{5}$$

Although the equivalent stress $\bar{\sigma}$ increases by the work hardening with deformation during the hydroforming, the increase in $\bar{\sigma}$ is comparatively small, and thus the left-hand side of Eq. (5) approximately becomes constant. Eq. (5) is rewritten by

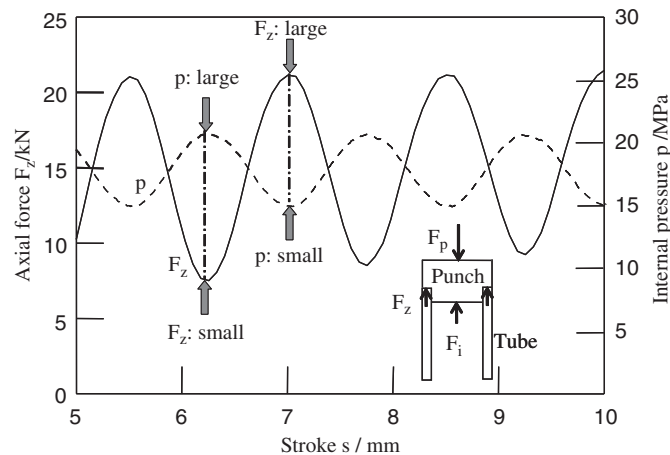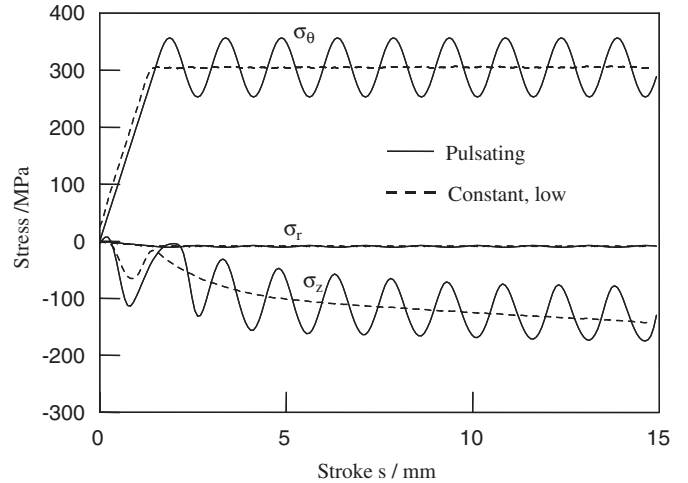$$\text{const.} \cong (\sigma_\theta - \sigma_z)^2 + \sigma_\theta^2 + \sigma_z^2. \tag{6}$$

Fig. 11. Oscillation of axial force and internal pressure during pulsating hydroforming for $p_0 = 17.7\,\text{MPa}$, $\Delta p = 3\,\text{MPa}$ and $\omega = 0.67\,\text{c/mm}$.

From the above equation, the difference between σ_θ and σ_z becomes almost constant during the oscillation. Since σ_θ is calculated from the internal pressure in Eq. (3), σ_θ and σ_z are oscillated synchronously with the internal pressure.

The cause of the uniform expansion in the pulsating hydroforming is explained from the change in stress components in Fig. 13. When the compressive σ_z and the tensile σ_θ are large and small, respectively, the small wrinkling appears, and then the wrinkling disappears due to the bulging for the small σ_z and the large σ_θ. By repeating this behaviour shown in Fig. 10, the uniform expansion is obtained, and thus the formability is improved by preventing the local thinning.

4.3. Finite element simulation

The effect of the oscillation of internal pressure was also examined from the finite element simulation. In the simulation, the rigid-plastic finite element method [12] was employed, and axi-symmetric deformation was assumed. The flow stress of the mild steel tube was measured from the tensile test as $\sigma = 510\varepsilon^{0.13}$ MPa. The coefficient of friction for the die was 0.05.

The deforming shapes of the bulging region obtained from the finite element simulation for the three pressure paths are shown in Fig. 14. The uniform expansion is obtained for the pulsating pressure, whereas the round bulge and wrinkling occur for the high and low constant pressures, respectively, as well as the experimental results shown in Fig. 3.

4.4. Large bulging length

In the above-mentioned results, the ratio of the bulging length to the diameter of the tube is 1.6. For a large bulging length, the effect of the pulsating pressure was examined from the experiment.

The formed tubes having a large bulging length obtained from the experiment for the three pressure paths are illustrated in Fig. 15, where the ratio of the bulging length to the diameter of the tube is 4.0. Even for the large bulging length, the uniform expansion was obtained in the pulsating pressure, whereas the round bulge and wrinkling occur for the high and low constant pressures, respectively.
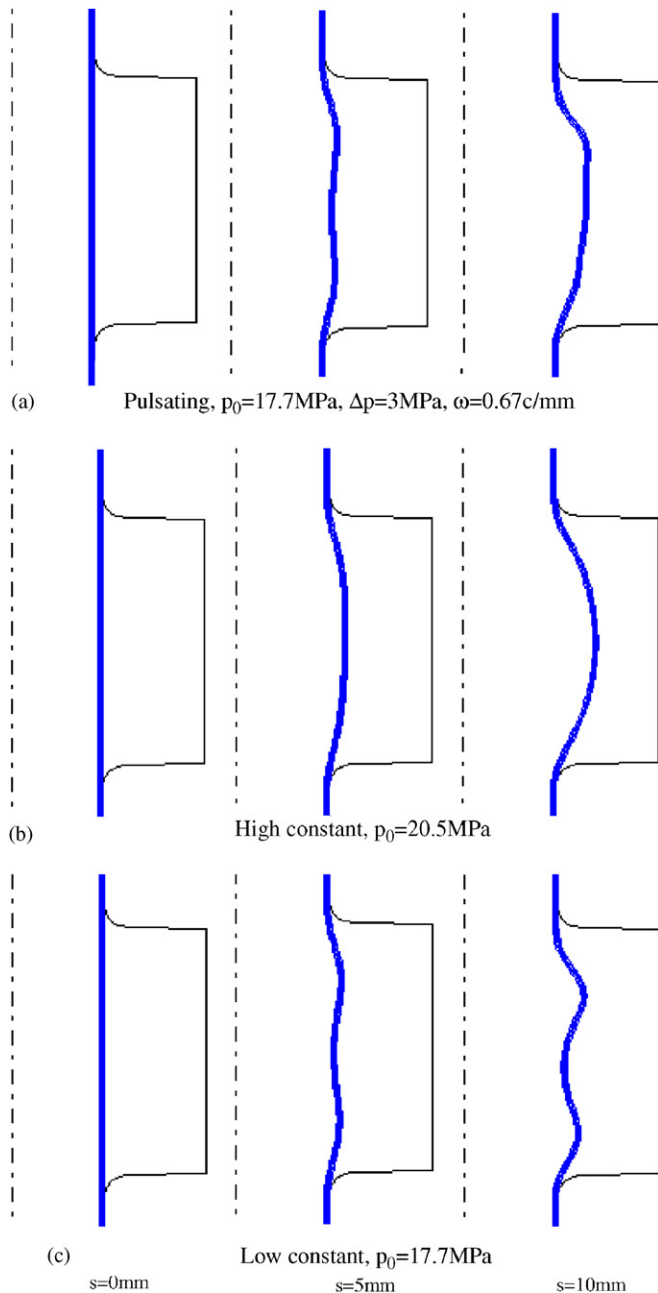

(a) Pulsating, p_0=17.7MPa, Δp=3MPa, ω=0.67c/mm

(b) High constant, p_0=20.5MPa

(c) Low constant, p_0=17.7MPa

s=0mm s=5mm s=10mm

Fig. 14. Deforming shapes of bulging region obtained from finite element simulation for three pressure paths.

Uniform expansion Round bulge Wrinkling

(a) Pulsating, p_0=18.6MPa, Δp=3MPa, ω=0.67c/mm

(b) High constant, p_0=21.7MPa
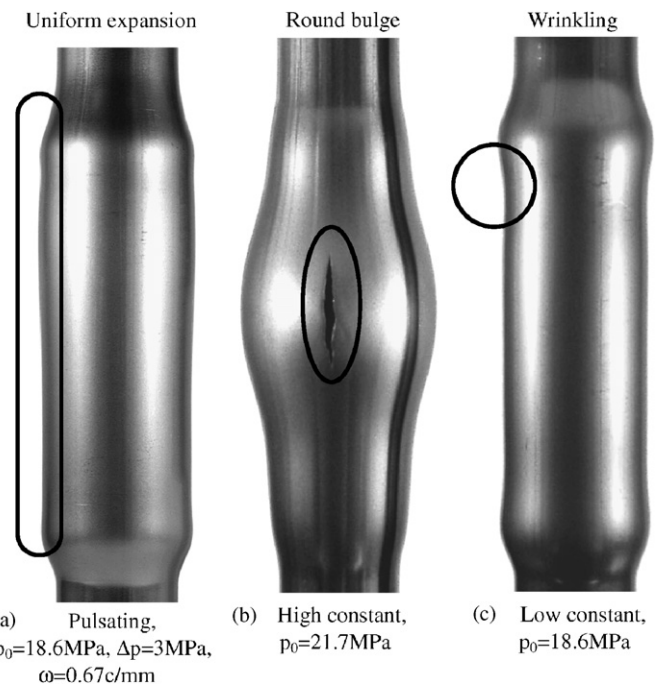
(c) Low constant, p_0=18.6MPa

Fig. 15. Formed tubes having large bulging length obtained from experiment for three pressure paths (ratio of bulging length to diameter of tube: 4.0).

5. Conclusions

The pulsating hydroforming is attractive for the improvement of the formability of tubes. The uniform expansion appearing in the pulsating hydroforming process is very different from the round bulge in the conventional hydroforming processes. The formability is largely improved by the uniform expansion without local thinning. Although the bulging region is not in contact with a die in the free bulging dealt with in the present study, the formability and shape accuracy of the products may be influenced by the deformation undergone before the contact with the die even in the die hydroforming processes.

References

[1] W. Rimkus, H. Bauer, M.J.A. Mihsein, Design of load-curves for hydroforming applications, Journal of Materials Processing Technology 108 (1) (2000) 97–105.

[2] J.-B. Yang, B.-H. Jeon, S.-I. Oh, Design sensitivity analysis and optimization of the hydroforming process, Journal of Materials Processing Technology 113 (1–3) (2001) 666–672.

[3] K.-J. Fann, P.-Y. Hsiao, Optimization of loading conditions for tube hydroforming, Journal of Materials Processing Technology 140 (1–3) (2003) 520–524.

[4] Y. Aue-U-Lan, G. Ngaile, T. Altan, Optimizing tube hydroforming using process simulation and experimental verification, Journal of Materials Processing Technology 146 (1) (2004) 137–143.

[5] M. Imaninejad, G. Subhash, A. Loukus, Loading path optimization of tube hydroforming process, International Journal of Machine Tools and Manufacture 45 (12–13) (2005) 1504–1514.

[6] T. Yogo, M. Ito, T. Mizuno, Digital master system of hammering hydroforming, Journal of the Japan Society for Technology of Plasticity 45 (527) (2004) 1022–1025 (in Japanese).

[7] K. Mori, A.U. Patwari, S. Maki, Improvement of formability by oscillation of internal pressure in pulsating hydroforming of tube, Annals of the CIRP 53 (1) (2004) 215–218.

[8] T. Hama, M. Asakawa, H. Fukiharu, A. Makinouchi, Simulation of hammering hydroforming by static explicit FEM, ISIJ International 44 (1) (2004) 123–128.

[9] K. Manabe, M. Amino, Effects of process parameters and material properties on deformation process in tube hydroforming, Journal of Materials Processing Technology 123 (2) (2002) 285–291.

[10] M. Murakawa, M. Jin, The utility of radially and ultrasonically vibrated dies in the wire drawing process, Journal of Materials Processing Technology 113 (1–3) (2001) 81–86.

[11] K. Mori, T. Maeno, M. Bakhshi-Jooybari, S. Maki, Measurement of friction force in free bulging pulsating hydroforming of tubes, in: P.F. Bariani et al. (Ed.), Advanced Technology of Plasticity 2005, Edizioni Progetto Padova, Padova, 2005, CD-ROM.

[12] K. Osakada, J. Nakano, K. Mori, Finite element method for rigid-plastic analysis of metal forming—formulation for finite deformation, International Journal of Mechanical Sciences 24 (8) (1982) 459–468.